A comparison of the circulation patterns over the Southwestern Atlantic Shelf driven by different wind stress climatologies

Elbio D. Palma,[1,2] Ricardo P. Matano,[3] Alberto R. Piola,[4] and Lina E. Sitz[1]

[1]   We compare the oceanic circulation patterns over the Southwestern Atlantic Shelf (SWAS) forced by nine different wind stress climatologies. The largest differences are observed in experiments forced with the *Hellerman and Rosenstein* [1983, hereafter HR83] and *Trenberth et al.* [1990, hereafter TR90] winds. HR83 shows a general northeastward flow near the shelf break. The TR90 results shows a bifurcating path south of ~40°S and a poleward flow north of 35°S. The most robust circulation patterns are a broad northward flow and the generation of coastal re-circulation cells in southern Patagonia and the development of a southward jet in the inner portion of the South Brazil Bight.   INDEX TERMS: 4219 Oceanography: General: Continental shelf processes; 4255 Oceanography: General: Numerical modeling; 4512 Oceanography: Physical: Currents. **Citation:** Palma, E. D., R. P. Matano, A. R. Piola, and L. E. Sitz (2004), A comparison of the circulation patterns over the Southwestern Atlantic Shelf driven by different wind stress climatologies, *Geophys. Res. Lett.*, *31*, L24303, doi:10.1029/2004GL021068.

1.   Introduction and Background

[2]   The Southwestern Atlantic Shelf (SWAS) extends from the Burdwood Bank, Argentina (55°S), to Cabo Frío, Brazil (23°S) (Figure 1). Along its western margin are the main industrial centers of South America: Rio de Janeiro, Sao Paulo, Montevideo and Buenos Aires, thus, the ocean circulation in this large portion of the world ocean influence the shelf environment of the most populated coastal region of the southern hemisphere. The wind-driven circulation consists of a general northward flow from the tip of Tierra del Fuego to approximately 40°S, a seasonally reversing circulation pattern from 37°S to 29°S [*Piola et al.*, 2000], and a southward alongshore flow farther north [*Castro and Miranda*, 1998]. Due to the scarcity of observations the general circulation over this region has been mostly inferred from numerical and analytical models forced with the HR83 wind stress climatology [e.g., *Forbes and Garraffo*, 1998; *Glorioso and Flather*, 1995; *Castro and Miranda*, 1998]. However, new climatologies derived from the results of

operational forecast models (e.g., European Centre for Medium-Range Weather Forecasts, ECMWF; National Centre for Environmental Prediction, NCEP), update of ship data [e.g., *da Silva et al.*, 1994], and satellite scatterometry (e.g., QuikSCAT) became available during the last decade. The differences among climatologies are particularly important for the oceanic circulation over the continental shelf because those regions are more influenced by the direct wind forcing than, for example, the neighboring western boundary regions. There are, however, no quantitative or qualitative estimates of the differences among wind stress climatologies over the southwestern Atlantic nor of their influence on the shelf circulation. In this article we compare the wind stress distribution over the southwestern Atlantic estimated by different available climatologies and assess their effect upon the circulation over the continental shelf.

2.   Wind Stress Climatologies

[3]   The wind stress climatologies used in our study differ in terms of the methodology used to produce them (e.g., the parameterization of the drag coefficient, height of wind speed retrieval, spatial resolution, etc.), the time period they covered and most important, the data sources employed in their production. The three largest data sources are in-situ observations collected from ships and buoys, re-analyses from Numerical Weather Prediction Centers (NWPC) simulations, and satellite observations (Table 1). To facilitate the comparison of scatterometer data (QuikSCAT) with the other wind products we re-sampled the NWPC data to cover the same period (1999–2001). The wind stresses were downloaded from freely available data libraries (http://ingrid.ldgo.columbia.edu/). No attempt was made to compute the wind stresses using the same parameterization for the drag coefficient or to evaluate the relative merits of each database. A brief overview of the general characteristics and time periods covered by the climatologies and the acronyms used in the simulations are given in Table 1. A more detailed description can be found in the original references.

[4]   For the purposes of comparison the wind data sets were divided in two groups: one based on long-term observations: HR83, DS94, SOC, TR90, ER15 and NC15 and the other on short-term observations: QU01, EC01 and NC01. To illustrate their differences we computed the annual mean wind stress in an alongshelf transect (Figure 1). There are distinct structures north and south of 37°S. In the south, the cross-shelf components of the winds are significantly stronger than the along-shelf components, while in the north both components have comparable magnitude (Figures 2a and 2b). The long-term climatologies show qualitatively similar structures, i.e., offshore winds south

[1]Departamento de Física, Universidad Nacional del Sur, Bahía Blanca, Argentina.
[2]Also at Instituto Argentino de Oceanografía (CONICET), Bahía Blanca, Argentina.
[3]College of Oceanic and Atmospheric Sciences (COAS), Oregon State University, Corvallis, Oregon, USA.
[4]Departamento de Oceanografía, Servicio de Hidrografía Naval, and Departamento de Ciencias de la Atmósfera y los Océanos, Universidad de Buenos Aires, Buenos Aires, Argentina.
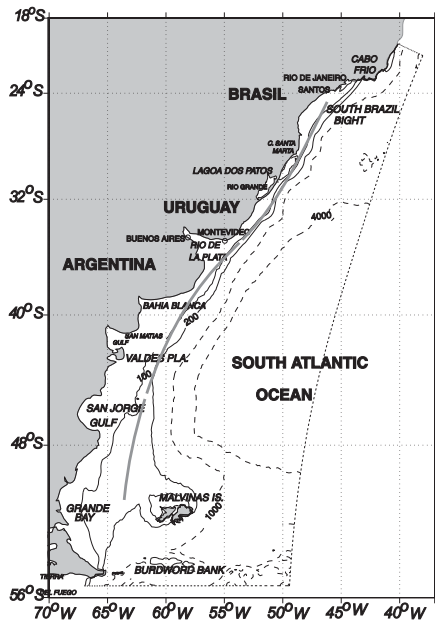
Figure 1. Map showing the bathymetry and geographical locations referred to in the text. The dotted line indicates the offshore limits of the model. The solid gray line indicates the along-shore cross section employed to decompose the wind stress components.

Figure 2. Climatological annual mean wind stress along the transect shown in Figure 1. The stress is projected normal and tangential to the transect, which can be thought as the cross-shore (top panels), and along-shore components (bottom panels). (a) and (b) long-term databases, (c) and (d) short-term databases.

of $\sim$35°S and onshore winds farther north. There are, however, quantitative differences in the southern stresses. The extremes are represented by DS94 and TR90, the former being approximately three times smaller than the later. The short-term climatologies show a general agreement of their cross-shelf components although differ in their along-shelf components e.g., the ECMWF reanalysis (EC01) and NCEP (NC01) (Figures 2c and 2d). These differences do not appear to be related to the shortness of the record because a similar discrepancy is observed in the long-term versions of both climatologies.

3. Model Description

[5] To investigate the sensitivity of the SWAS circulation to the wind stress climatologies we did a series of numerical experiments using the Princeton Ocean Model (POM) [*Blumberg and Mellor*, 1987]. The model uses a curvilinear horizontal grid to cover a domain that extends from 55°S to 20°S and from 70°W to 40°W (Figure 1). This grid has an average resolution of 7.5 km in the alongshore direction, 10 km in the cross-shore direction and 25 vertical sigma-
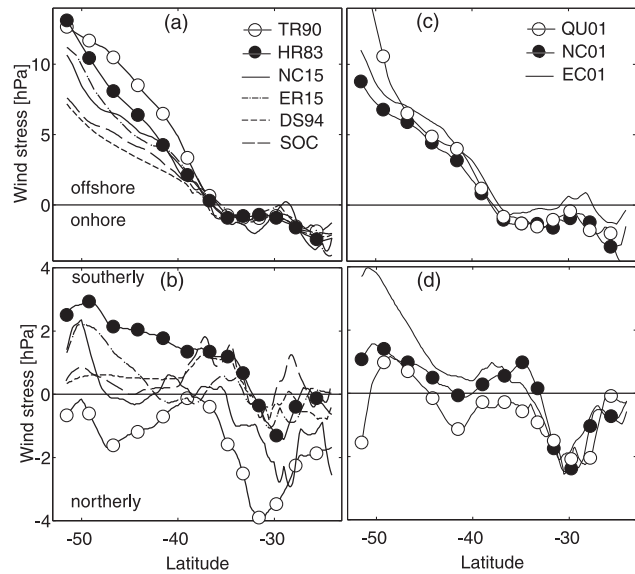
levels. The model was initialized with constant temperature and salinity and forced with the annual average wind stress from the different climatologies. To incorporate the frictional effects of the tides, which are particularly important in the southern portion of the domain, the model was also forced at its open boundaries with the five largest tidal constituents extracted from the Oregon State University Global Tidal Model [*Egbert et al.*, 1994]. The numerical experiments were started from scratch, spun-up for a 30-day period, and run in prognostic mode for an additional 60-days period. At the end of each run the tidal residual currents (previously calculated from a tides-only experiment), were subtracted and the 60-day average used for analysis.

4. Results

[6] The largest differences in circulation patterns corresponded to the experiments forced with HR83 and TR90 (Figure 3). The HR83 experiment shows a general northward flow, largely concentrated near the shelf break that includes coastal re-circulation cells near 53°S and 47°S. The TR90 experiment shows an intensification of the circulation

Table 1. Wind Stress Data Set Information Showing the Temporal and Spatial Resolution of the Original Wind Products Used in This Study

| Wind Stress	Source	Grid	Period	Reference
HR83	Marine observations	2° × 2°	1870–1976	*Hellerman and Rosenstein* [1983]
DS94 (COADS)	Marine observations	1° × 1°	1945–1989	*da Silva et al.* [1994]
SOC	Marine observations	1° × 1°	1980–1993	*Josey et al.* [1996]
TR90 (ECMWF)	Analysis product	2.5° × 2.5°	1980–1986	*Trenberth et al.* [1990]
ER15 (ECMWF)	Analysis product	2.5° × 2.5°	1979–1993	*Garnier et al.* [2000]
NC15 (NCEP)	Analysis product	1.87° × 1.87°	1979–1993	*Kalnay et al.* [1996]
QU01(QuikSCAT)	Scatterometer product	1° × 1°	1999–2001	Jet Propulsion Laboratory
EC01 (ECMWF)	Analysis product	1° × 1°	1999–2001	ECMWF
NC01 (NCEP)	Analysis product	1.87° × 1.87°	1999–2001	*Kalnay et al.* [1996]
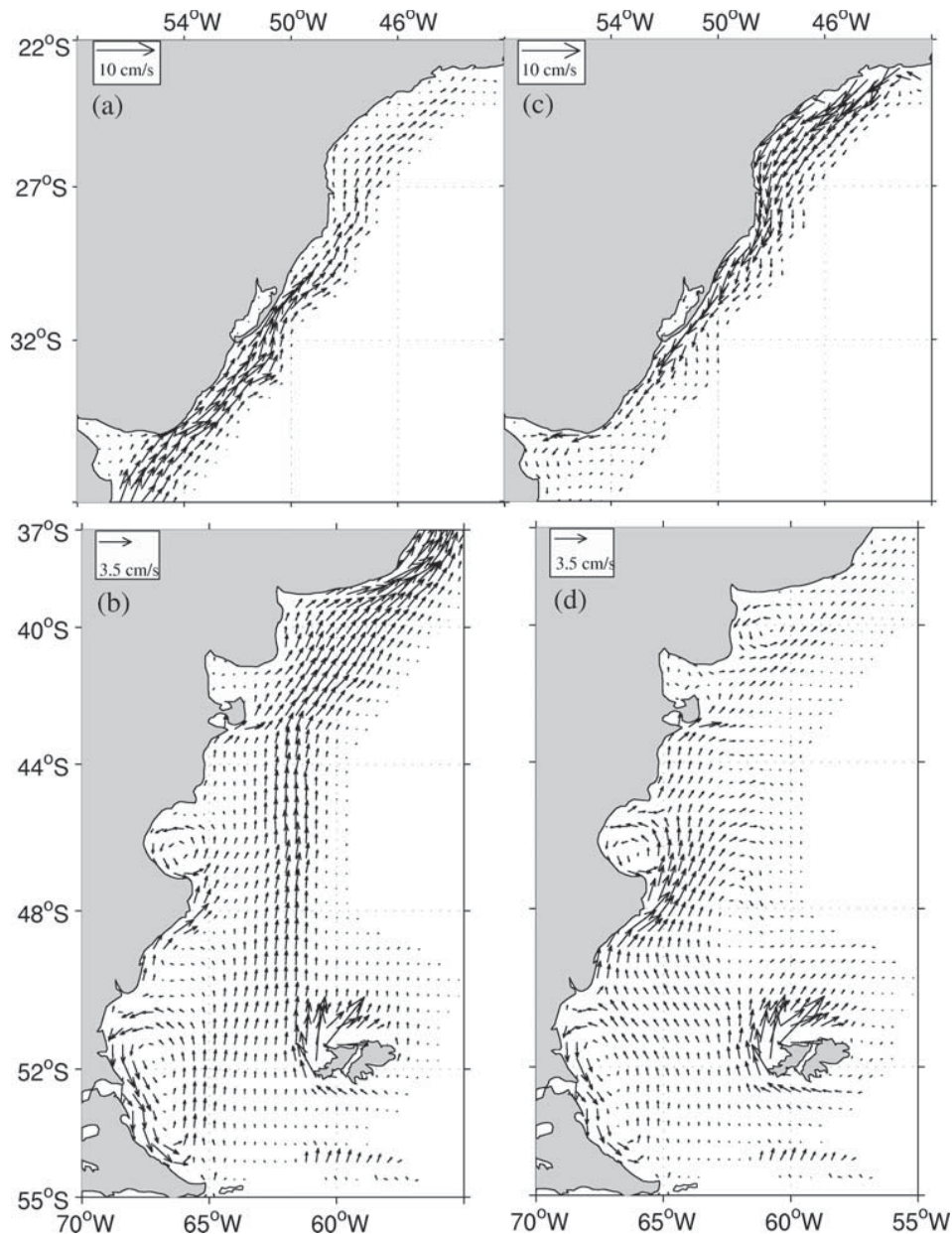
Figure 3. Annual mean depth averaged velocity vectors computed from the model forced by the (a) and (b) *Hellerman and Rosenstein* [1983] annual mean wind stress; (c) and (d) *Trenberth et al.* [1990] annual mean wind stress. Note the difference in vector scale among top and bottom panels.

near the coast in the southern portion of the shelf and a poleward flow north of ~35°S. The most robust features of these two experiments, and also of the experiments forced with the other climatologies, are the re-circulation cells of southern Patagonia and the intensification of the circulation in the westward side of the Malvinas Is. The largest transports of the re-circulation cells were observed in the experiments forced with the NC15 and ER15 winds and the smallest with the DS94, HR83 and TR90 winds.

[7] To quantify the differences among all the experiments we computed the along-shelf and cross-shelf transports along the sections indicated in Figure 1. The largest differences of the along-shelf transport correspond to the experiments forced with the HR83 and TR90 (Figures 4a and 4b).

HR83 shows a northward flow over most of the shelf domain with a maximum of ~0.6 Sv (1 Sv = 1×10^6 m^{3}s^{-1}) near 51°S. The experiment forced with the TR90 winds shows southward flow north of ~36°S. The alongshelf transports of the experiments forced with DS94, SOC, and NC15 are qualitatively similar to those of HR83, although their magnitudes are generally less than a half of those of HR83. The along-shelf transport of the experiment forced with the ER15 winds is the most similar to the TR90, but it shows an increment of the northward transport north of 46°S. The differences in the cross-shelf transport are smaller than those in the along-shelf transport. All the experiments show an offshore cross-shelf transport south of ~43°S and inshore transport in the latitude band between 43°S and
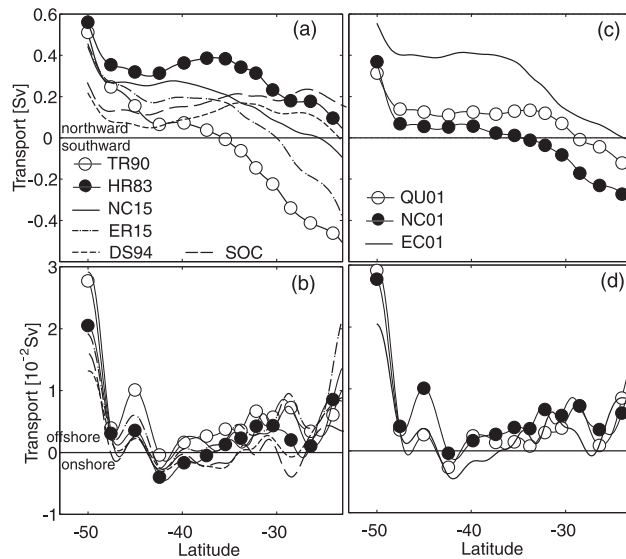
Figure 4. Northward transport (in Sv) across the sections normal to the along-shelf transect indicated in Figure 1 (top panels), and offshore transport through the 200 m isobath (bottom panels). The cross sections in the top panels run from the coast to the 200 m isobath. (a) and (b) long-term databases, (c) and (d) short-term databases.

37°S. The latter is the region where the coastline orientation shifts to the northeast and the shelf width starts to narrow. DS94, SOC, and HR83 show the broadest band of inshore transport, between 43°S and 34°S, which contributes to the increase of northward transport north of 45°S that is absent, or nearly negligible, in the other experiments.

[8] The currents fields obtained from simulations forced with scatterometer winds (QU01) are similar to the experiment NC01. The bulk of the northward flow, in the southern shelf, is concentrated near the shelf break. The alongshelf transport is less than 0.3 Sv and qualitatively comparable in both experiments (Figure 4c). In contrast, the mean transport in the EC01 experiment is channeled within the shelf region, shows little offshore exchange and is four times larger than QU01. The northward penetration of southern shelf waters is also larger for EC01 (and comparable to HR83 and DS94) and weaker for NCO1. QUO1 and NCO1, like most long-term climatologies, exhibit a continuous southward flow in the inner South Brazil Bight. With the exception of a small region near 43°S the cross-shelf transport in all the experiments is offshore, with maximum differences in southern Patagonia, where the outflow of shelf waters generated by NC01 is two times larger than those forced by QU01 and EC01 (Figure 4d).

5. Summary and Conclusions

[9] Our results show that there are important differences among the most widely used wind stress climatologies and that those differences are likely to be important for the circulation and water mass structure of the shelf region. Some of the differences in the simulated circulations can be ascribed to the magnitude of the winds. HR83 and DS94, for example, show a similar spatial structure but different

magnitudes. Similarly, TR90 and ER15 used different levels for wind speed retrieval (1000db for TR90 and 10 m for ER15) and consequently there is a much weaker shelf response under ER15 in southern Patagonia.

[10] The most important differences induced by a particular wind stress however, are those related to the spatial structure of the winds, which can be attributed to differences in the data source or the time span they covered. Ocean simulations forced with the TR90 winds, for example, show offshore transport all along the SWAS while those forced with the HR83 have a substantial onshore transport between 43°S and 32°S. The water mass characteristics of the shelf in the former case would be determined by inflows from high and mid latitudes while in the later case they will be substantially influenced by entrainments of waters from the Brazil/Malvinas confluence region. These differences are related to the fact that TR90 has a larger southward alongshelf component (Figure 2b).

[11] Although we do not have in-situ observations to evaluate the different wind stress climatologies, the ocean circulation patterns generated by the HR83, seem to be the least realistic of all. In the northern portion of the SWAS, for example, this climatology generated an equatorward mass flux that is in contradiction with existing observations [*Castro and Miranda*, 1998]. The circulation patterns produced by the short-term climatologies show regional differences north and south of ~35°S. In the south QUO1 and NCO1 produce similar circulation patterns, while in the north the results of QUO1 and ECO1 are in better agreement (Figure 4c). In spite of all the differences our numerical experiments have also shown the existence of robust patterns of circulation such as the broad northward flow in the southern Patagonian shelf (south of ~50°S, Figure 2), the re-circulation cells near the Grande Bay and the San Jorge Gulf, and the southward alongshore flow in the South Brazil Bight.

References

Blumberg, A. F., and G. L. Mellor (1987), A description of a three-dimensional coastal ocean circulation model, in *Three-Dimensional Coastal Ocean Models*, *Coastal Estuarine Sci. Ser.*, vol. 4, edited by N. Heaps, pp. 1–16, AGU, Washington D. C.

Castro, B. M., and L. B. Miranda (1998), Physical oceanography of the western Atlantic continental shelf located between 4N and 34S, in *The Sea*, vol. 11, edited by A. R. Robinson and K. H. Brink, pp. 209–251, John Wiley, Hoboken, N. J.

da Silva, A. M., C. C. Young, and S. Levitus (1994), *Atlas of Surface Marine Data 1994*, vol. 1, *Algorithms and Procedures*, *NOAA Atlas NESDIS*, vol. 6, Natl. Oceanic and Atmos. Admin., Silver Spring, Md.

Egbert, G. D., A. F. Bennet, and M. G. G. Foreman (1994), TOPEX/POSEIDON tides estimated using a global inverse model, *J. Geophys. Res.*, 99, 24,821–24,852.

Forbes, M. C., and Z. D. Garraffo (1998), A note on the mean seasonal transport on the Argentinean shelf, *J. Geophys. Res.*, 93, 2311–2319.

Garnier, E., B. Barnier, L. Siefridt, and K. Beranger (2000), Investigating the 15 years air-sea climatology from the ECMWF re-analysis project as a surface boundary condition for ocean models, *Int. J. Climatol.*, 20, 1563–1673.

Glorioso, P. D., and R. A. Flather (1995), A barotropic model of the currents off SE South America, *J. Geophys. Res.*, 100, 13,427–13,440.

Hellerman, S., and M. Rosenstein (1983), Normal monthly wind stress over the world ocean with error estimates, *J. Phys. Oceanogr.*, *13*, 1093–1104.

Josey, S. A., E. C. Kent, D. Oakley, and P. K. Taylor (1996), A new global air-sea heat and momentum flux climatology, *Int. WOCE Newsl.*, *24*, 3–5.

Kalnay, E., et al. (1996), The NCEP/NCAR reanalysis project, *Bull. Am. Meteorol. Soc.*, *77*, 437–471.

Piola, A. R., E. J. D. Campos, O. O. Moller, M. Charo, and C. Martinez (2000), Subtropical shelf front off eastern South America, *J. Geophys. Res.*, *105*, 6565–6578.

Trenberth, K. E., W. G. Large, and J. G. Olson (1990), The mean annual cycle in global wind stress, *J. Phys. Oceanogr.*, *20*, 1742–1760.

————————————

R. P. Matano, College of Oceanic and Atmospheric Sciences (COAS), Oregon State University, Corvallis, OR, USA.

E. D. Palma and L. E. Sitz, Departamento de Física, Universidad Nacional del Sur, Avda. Alem 1254, 8000 Bahía Blanca, Argentina. (uspalma@criba.edu.ar)

A. R. Piola, Departamento de Oceanografía, Servicio de Hidrografía Naval, Buenos Aires, Argentina.